Smart electrode array for cochlear implants

Ahmad Itawi, Sofiane Ghenna, Guillaume Tourrel, Sébastien Grondel, Cedric Plesse, Giao Tran Minh Nguyen, Frederic Vidal, Yinoussa Adagolodjo, Lingxiao Xun, Gang Zheng, et al.

SMART ELECTRODE ARRAY FOR COCHLEAR IMPLANTS

Ahmad Itawi[1], Sofiane Ghenna[1], Guillaume Tourrel[2], Sébastien Grondel[1], Cédric Plesse[3], Tran Minh Giao Nguyen[3], Frédéric Vidal[3], Yinoussa Adagolodjo[4], Lingxiao Xun[4], Gang Zheng[4], Alexandre Kruszewski[4], Christian Duriez[4], and Eric Cattan[1]

[1]Univ. Polytechnique Hauts-de-France, CNRS, Univ. Lille, UMR 8520 - IEMN, Valenciennes, France.

[2]Oticon Medical, Research & Technology, Vallauris, France.

[3] CY Cergy Paris Université, LPPI, EA2528, Cergy-Pontoise, France and

[4]DEFROST, Univ. Lille, Inria, CNRS, Centrale Lille, UMR 9189 CRIStAL, Lille, France.

ABSTRACT

Cochlear implants made of standard silicone electrode array (EA) are currently used to stimulate the auditory nerve of patients' cochlea. The implants have a proximal diameter of 0.5mm and 2~3cm long composed of 20 bulk platinum electrodes and connection wires (Ø 25µm). Due to their stiffness and passive nature, the most difficult task during implant surgery is inserting the EA properly into the tympanic ramp of the patient's cochlea, often leading to trauma or incomplete insertion. In this work, we developed an original smart EA for efficient insertion. This prototype has a lower stiffness and functionalized with an electronic conducting polymer based micro-actuators able to bend under low electrical voltage stimulation. This prototype is expected to reduce the friction forces during insertion, allow better control of the insertion process, facilitate the work of the surgeon and decrease the probability of trauma.

KEYWORDS

Cochlear electrode array, electronic conducting polymer, actuator

INTRODUCTION

At present, commercially available cochlear implant electrode arrays are all manually assembled, consisting of a wire-bundle design with 12–26 electrodes, a length of 16–30mm, and an electrode surface area of 0.12–1.5mm^2. Platinum or platinum-iridium alloy electrode arrays are hand-fabricated and assembled from a bundle of fine wires. The most important factor when designing an electrode array is to provide an atraumatic insertion solution in order to prevent causing damage to any of the intra-cochlear structures. For example, the damage caused by the insertion of the cochlear implant may be a translocation from the scala tympani (ST) to the scala vestibuli. The implementation of EAs is particularly challenging because of the friction between the conventional electrode and the lateral wall of the ST. This is partly due to the mechanical mismatch between the stiffness of the materials, e.g., silicone (Young's modulus E ≈ 1 - 10MPa), platinum-iridium (Young's modulus E ≈ 170GPa), constituting such probes and the softness of the walls of the cochlea (E ≈ 10kPa). This mechanical mismatch, which can reach seven orders of magnitude, leads to irreversible tissue damage. It is also necessary that the structure of the EA facilitates a complete insertion, therefore having the array homogeneously placed along the lateral wall in close proximity with the basilar membrane is essential (Figure 1). A motorized insertion tool, external to the ear, is currently used to push a blunt pin into an insertion tube and eject the EA into the cochlea.

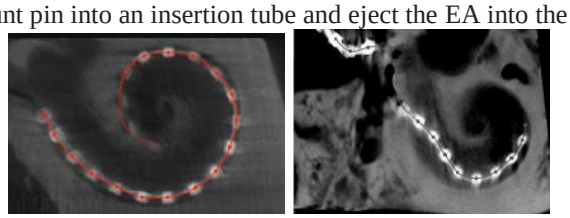

Figure 1: Computed tomography scan post-insertion of a cochlear implant; Left: successful insertion allowing activation of all electrodes; Right: incomplete insertion.

Research work is trying to get out of traditional manufacturing methods by moving towards the use of skills in the field of flexible electrodes made from microfabrication technologies. This evolution is driven in large part by the progress made in the field of stimulation electrodes for the brain [1], [2]. The use of flexible probes achieves better compliance with the surrounding tissues of the cochlea whereas simultaneously minimal friction improves the ST-EA interface. Thin-film EAs have already been developed from boron diffusion silicon substrate designs [3], [4] and flexible polymer substrate designs [5]. The state-of-the-art cochlear thin-film EAs developed by Johnson and Wise contains 32 electrodes on an 8-mm-long array in a curve-controlled shape with a system-level ASIC [6]. Despite these significant advances, none of the MEMS electrodes is currently used in commercial cochlear implants applications for humans. Notice however that friction along the lateral wall inducing jamming upon entry into the cochlea is not discussed nor considered for very flexible EA. Moreover, to our knowledge, micro-actuated EA for microfabricated thin cochlear implants do not exist. Consequently, electronic conducting polymer (ECP) based micro-actuators have been chosen because of their high stress per unit mass at

low voltage (2V) [7, 8]. For completeness, it should also be recalled that current catheters fabricated with ECP [9, 10] are not suitable for integrating an EA thin film.

RESULTS AND DISCUSSION

The bending stiffness of a traditional implant EA results primarily from the platinum electrode and the electrical connection wires. The measured stiffness at 3.5mm of the clamping point is close to 60µN/µm (Figure 2a). This stiffness is 300 times lower and reduced to 0.2µN/µm, at the same distance, by removing bulk platinum electrodes and wires and by keeping only the silicone carrier. In this last situation, the blocking forces produced by poly(3,4-ethylenedioxythiophene):poly(styrene sulfonate) (PEDOT:PSS) based micro-actuator are optimized by changing the thicknesses of each layer of the micro-actuator (Figure 2b).

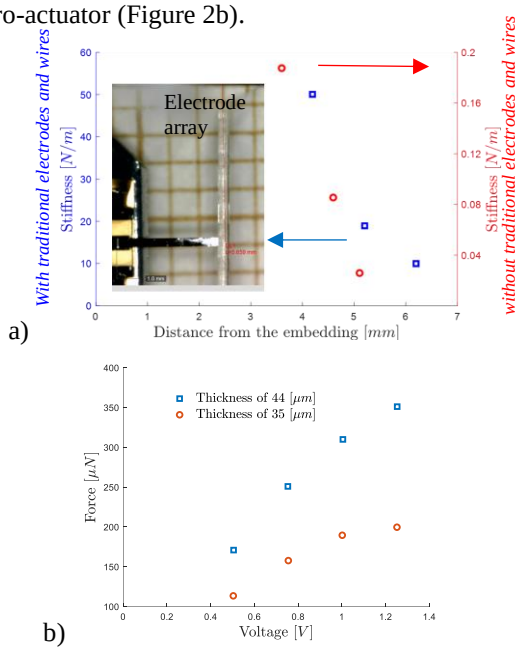

Figure 2: a) Comparison of the stiffness for a round silicon bar with (blue points)/without (red points) traditional platinum electrodes and connection wires, b) Optimization of the micro-actuator thickness to obtain enough force to bend the EA.

The micro-actuators composed of a nitrile butadiene rubber/poly(ethylene oxide) (NBR-PEO) ion storage membrane sandwiched between two electroactive PEDOT:PSS-PEO layers were fabricated using the layer stacking method [11], [12]. The PEDOT:PSS-PEO casting solutions were obtained by mixing PEO (poly(ethylene oxide)) with an aqueous dispersion of PEDOT:PSS (40wt% with respect to the final electrode). The resulting solution was cast (0.1ml.cm^{-2}) onto a glass slide and placed on a heating plate at 50°C to evaporate the water. The ion storage membrane is based on a semi-interpenetrating polymer network layer composed of a PEO network (50wt%) and linear NBR (50wt%). First, the NBR solution was prepared by dissolving NBR in cyclohexanone to obtain a concentration of 20wt%. The PEO is added to the NBR solution. The radical initiator DCPD (3wt% with respect to the PEO network) was then added to the solution. The final solution was stirred until complete homogenization and degassed. During the next step, the reactive mixture was spin coated (1500rpm – 1000rpm/s – 30s) onto the first PEDOT:PSS-PEO electrode layer and pre-polymerized in a closed annealing chamber under continuous nitrogen flow for 45min at 50°C to initiate the formation of the PEO network. The second PEDOT:PSS-PEO electrode was fabricated on top of the PEDOT:PSS-PEO/NBR-PEO bilayer in the same way as the first electrode: new solutions were prepared, cast, and solidified at 50°C by evaporating the water. The resulting trilayer micro-actuators were then placed in a closed annealing chamber and the final heat treatment was carried out at 50°C for 3 h followed by post-curing at 80°C for 1 h under a continuous nitrogen flow. Finally, the micro-actuator is swollen in 1-ethyl-3-methylimidazolium bis(trifluoro-methanesulfonyl) -imide electrolyte.

The micro-actuator force can reach 350µN at a distance of 2mm from the embedding point under 1.25V (Figure 2b). Depending on the applied voltage, the induced displacement is enough to move the silicone carrier to a few hundred micrometers in order to separate the implant from the lateral wall and reduce friction and capillary effect.

The overall design of the traditional stimulation of EA has been fully amended to reduce the EA stiffness. The proposed microsystem is an addition of a very thin and flexible EA, one or several distributed ECP based micro-actuators and a Polydimethylsiloxane (PDMS) carrier (Figure 3a). For new EA, a SU-8 thin-film was microfabricated with a density of 20 electrode contacts along a 25mm in length. (Figure 3c). The neutral line is used to run the 10µm wide gold lines.

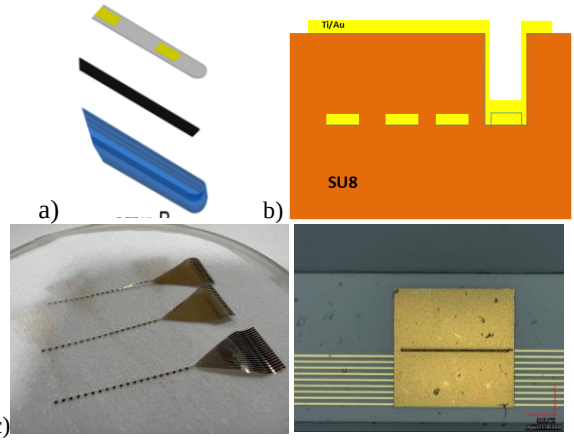

Figure 3: a) Exploded view of the new prototype, b) cross-sectional drawing showing microfabrication steps c) SU-8 electrode arrays with detailed view of an electrode contact and connecting lines.

The microfabrication process is done as follows: first, Omnicoat is spun coated to create a sacrificial layer to remove flexible EA from the silicon substrate at the end of the process. Then 7 µm thickness of SU-8 photoresist is deposited and UV insolated to define the shape of the EA. The first metallic layer (Ti/Au - 20nm/0.5µm) was deposited by evaporation. Gold and titanium layers circuit were defined by chemical etching: KI:I_2:H_2O and BOE 7.1 respectively. The second SU-8 layer with the same thickness is spin-coated to place the metal circuit in the neutral plane. The opening of SU-8 is made and the second metal layer is processed like the previous one to make the interconnect. Each site comprises a 0.45mm×0.40mm square gold electrode to maximize the surface in front of the basilar membrane (Figure 3b). With a total thickness of 14µm the new EA stiffness is 0.6µN/µm at 2mm, which corresponds to a decrease of a factor of 100 compared to traditional electrode arrays, and can be reduced more by decreasing the thicknesses of the two SU-8 layers: for example, the stiffness is reduced to 0.2µN/µm when the thickness is decreased at 10µm. The measured resistances at the first and last electrodes are around 45±5Ω and 300±20Ω respectively which is consistent with the theoretically calculated value.

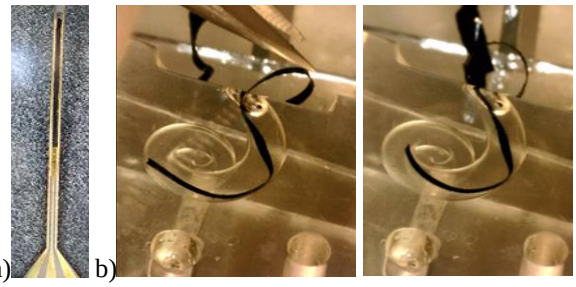

Figure 4: a) ECP-based micro-actuators clamped in a SU-8 micro-structure with integrated gold remote contacts. The actuator is a beam of 6 mm length and 300 µm wide. b) Actuation principle (without EA) inside a transparent 3D printed cochlea model. Actuator "off" on the left and "on" on the "right".

However, its insertion into a transparent 3D printed cochlea model does not exceed 180°due to the friction of the SU-8 beam edges on the lateral wall of the 3D printed cochlea model. Indeed, this friction causes an “accordion” effect of the EA at the entrance of the cochlea preventing adequate thrust. To actuate the EA in three different points, the smallest ECP-based micro-actuators (6x0.3mm^2) integrated ever used were clamped to a SU-8 micro-structure with integrated gold remote contacts by using a microfabrication method described in [13] (Figure 4a). The tests with this integrated micro-actuator inside the cochlea are currently in progress. The micro-actuator can also be envisaged as a laser cutting beam of 2.5cm with a width of 0.5mm used for an actuation along all the EA. With the appropriate electrical excitation, we have already demonstrated that the laser cutting micro-actuator can move its tip from a position near the lateral wall of the cochlea model to the inner wall, when it is full of glycerin to simulate the perilymph (Figure 4b).

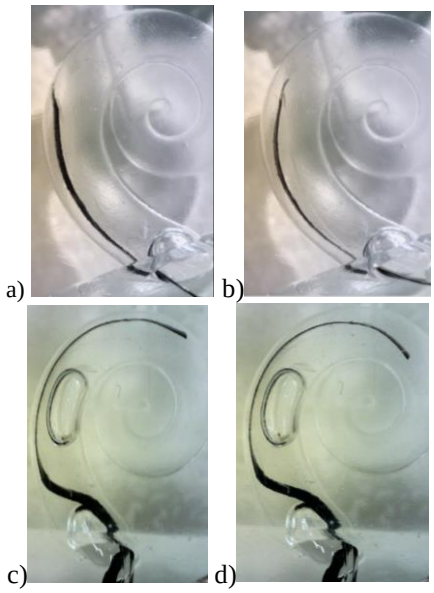

Figure 5: Micro-actuator added along an EA a) and b) and PDMS U-shape carrier without reservoir c) and d) to detach them from the lateral wall a) and d) off, b) and c) on.

It is then easier to push and move forward the actuator in the cochlea but its flexibility also produces the accordion effect. To limit this effect, the thickness of the micro-actuator has been increased to 70µm. Tests performed with this micro-actuator added along an EA and PDMS carrier (Figure 5a, b, c and d) have demonstrated that it could be successfully detached from the lateral wall.

At the same time, a new PDMS U-shape carrier has been prepared with small reservoirs inside the PDMS. The latter have been filled with SU-8 in order to add rigidity along the thrust axis while keeping bending flexibility thanks to the PDMS reservoir separations (Figure 6a). Note also that SU-8 added prevents the PDMS carrier from folding like an accordion. With this solution, a successful insertion in the 3D printed cochlea model with an angle of 490° has been obtained (Figure 6b).

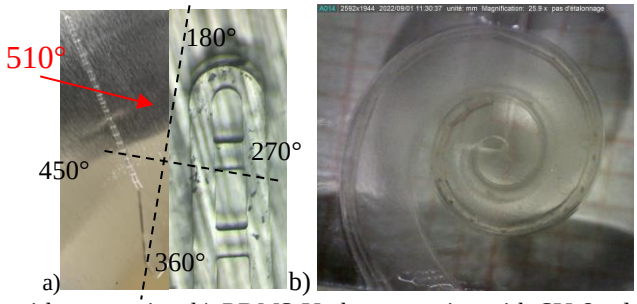

Figure 6: a) PDMS U-shape with reservoirs, b) PDMS U-shape carrier with SU-8 added. b) Insertion into 3D printed cochlea model with a progression to an angle of 490°.

In parallel, using the SOFA framework, we performed a simulation of the process of EA insertion into the cochlea based on the finite element (FE) method and Cosserat's theory [15]. To manage the different interactions that may appear between the EA and the cochlea, we have chosen a formulation based on Lagrangian constraints using Signorini's law for contact and Coulomb's law for friction. Figure 7 shows the intensity of the frictional force as the EA progresses through the cochlea. The calculation of this intensity depends on the friction parameter between the EA and the cochlea. A first empirical study was therefore carried out by comparing the forces obtained at the base of the EA during the simulation and that recorded by a sensor placed on the real electrode. The friction parameters that offer a force profile close to that recorded by the sensor, throughout the insertion procedure, were considered for the simulation of this new EA. We saw a 30% drop in max strength using these settings on the new EA.

The objective of this simulation is therefore to determine the regions of high friction between the EA and the cochlea. Then provide an optimal distribution of micro-actuators in the EA to further reduce the frictional force and avoid blockages during insertion.

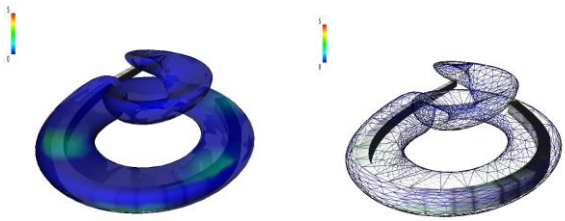

Figure 7: Simulation of cochlear implant insertion to identify contact areas in the cochlea at different stages of the process.

CONCLUSIONS

The main aim of this study was to propose a solution to reduce the friction forces against the lateral cochlea wall during implant insertion by the surgeons. To solve this problem, the first idea has been to reduce the stiffness of the cochlear implant. However, it should be noted that by reducing drastically the stiffness, the implant will set in the accordion and lock at the entrance to the cochlea. To counterbalance this drawback, we have thereafter proposed to integrate ECP micro-actuators on the cochlear implant in order to allow its bending during the insertion. Using such original approach, we have demonstrated that the EA stiffness of the cochlear implant could be reduced by 100 and that the forces necessary for its bending became compatible with forces developed by ECP micro-actuators. These forces are currently on the order of 400µN at 2mm from the clamping point. Next, on the one hand, the EAs have been designed to put gold electrode as close as possible to the basilar wall of the cochlea, with large electrode surfaces of 0.2µm^2 and a low resistance whereas on the other hand micro-actuators have been added to the EA and to the PDMS carrier. Then, it has successfully been shown that the use of micro-actuators allowed first the implant separation from the lateral wall of the cochlea under an electrical voltage of 1.5V and second improved its progression through the cochlea. To improve the efficiency of the proposed solution, an original PDMS U-shape holder with reservoirs has been finally designed. In fact, the addition of SU-8 in the reservoir as well the UV cure increase the EA stiffness and then prevent the implant from folding like an accordion. A successful insertion in the 3D printed cochlea model with an angle of 490° has been obtained which demonstrates the interest of the proposed solution. Future work will be focused on two aspects to improve the insertion efficiency. The first deals with the optimization of the microactuators distribution thanks to the simulation whereas the second concerns the possibility of using a closed loop control [14] during insertion.

ACKNOWLEDGEMENTS

This work was partly financially supported by the French National Research Agency with RENATECH, and ROBOCOP (ANR PRCE 19 CE19) projects.

REFERENCES

[1] E. Patrick, M. Ordonez, N. Alba, J. C. Sanchez, and T. Nishida, “Design and fabrication of a flexible substrate mieroelectrode array for brain machine interfaces,” in *Annual International Conference of the IEEE Engineering in Medicine and Biology - Proceedings*, 2006, pp. 2966–2969.

[2] C. Cointe *et al.*, “Scalable batch fabrication of ultrathin flexible neural probes using a bioresorbable silk layer,” *Microsystems Nanoeng.*, vol. 8, no. 1, Dec. 2022.

[3] J. Wang and K. D. Wise, “A hybrid electrode array with built-in position sensors for an implantable MEMS-based cochlear prosthesis,” *J. Microelectromechanical Syst.*, vol. 17, no. 5, pp. 1187–1194, 2008.

[4] N. S. Lawand, P. J. French, J. J. Briaire, and J. H. M. Frijns, “Design and fabrication of stiff silicon probes: A step towards sophisticated cochlear implant electrodes,” *Procedia Eng.*, vol. 25, pp. 1012–1015, 2011.

[5] Y. Xu, C. Luo, F. G. Zeng, J. C. Middlebrooks, H. W. Lin, and Z. You, “Design, fabrication, and evaluation of a parylene thin-film electrode array for cochlear implants,” *IEEE Trans. Biomed. Eng.*, vol. 66, no. 2, pp. 573–583, Feb. 2019.

[6] A. C. Johnson and K. D. Wise, “An active thin-film cochlear electrode array with monolithic backing and curl,” *J. Microelectromechanical Syst.*, vol. 23, no. 2, pp. 428–437, 2014.

[7] D. Zhou *et al.*, “Solid state actuators based on polypyrrole and polymer-in-ionic liquid electrolytes,” *Electrochim. Acta*, vol. 48, no. 14-16 SPEC., pp. 2355–2359, 2003.

[8] J. D. Madden, D. Rinderknecht, P. A. Anquetil, and I. W. Hunter, “Creep and cycle life in polypyrrole actuators,” *Sensors Actuators, A Phys.*, vol. 133, no. 1, pp. 210–217, 2007.

[9] A. Mazzoldi and D. De Rossi, “Conductive-polymer-based structures for a steerable catheter,” *Smart Struct. Mater. 2000 Electroact. Polym. Actuators Devices*, vol. 3987, p. 273, 2000.

[10] T. Shoa, J. D. Madden, N. Fekri, N. R. Munce, and V. X. D. Yang, “Conducting Polymer Based Active Catheter for Minimally Invasive Interventions inside Arteries,” *30th Annu. Int. IEEE EMBS Conf.*, pp. 2063–2066, 2008.

[11] K. Rohtlaid, G. T. M. Nguyen, C. Soyer, E. Cattan, F. Vidal, and C. Plesse, “Poly(3,4-ethylenedioxythiophene):Poly(styrene sulfonate)/Polyethylene Oxide Electrodes with Improved Electrical and

Electrochemical Properties for Soft Microactuators and Microsensors," *Adv. Electron. Mater.*, vol. 5, no. 4, 2019.
[12] T. N. Nguyen *et al.*, "Ultrathin electrochemically driven conducting polymer actuators: fabrication and electrochemomechanical characterization," *Electrochim. Acta*, vol. 265, pp. 670–680, 2018.
[13] L. Seurre *et al.*, "Demonstrating Full Integration Process for Electroactive Polymer Microtransducers to Realize Soft Microchips," in *Proceedings of the IEEE International Conference on Micro Electro Mechanical Systems (MEMS)*, 2020.
[14] L. Xun *et al.*, "Modeling and Control of Conducting Polymer Actuator," *IEEE/ASME Trans. Mechatronics*, accepted for inclusion in a future issue, 2022.
[15] Y. Adagolodjo et al "Coupling numerical deformable models in global and reduced coordinates for the simulation of the direct and the inverse kinematics of Soft Robots" IEEE Robotics and Automation Letters, 2021.

CONTACT

*S. Ghenna, tel: +33(0)327 51 14 45; Sofiane.ghenna@upf.fr